Wildfire prevention through prophylactic treatment of high-risk landscapes using viscoelastic retardant fluids

Anthony C. Yu[a], Hector Lopez Hernandez[a], Andrew H. Kim[b], Lyndsay M. Stapleton[c], Reuben J. Brand[d], Eric T. Mellor[d], Cameron P. Bauer[d], Gregory D. McCurdy[e], Albert J. Wolff III[e], Doreen Chan[f], Craig S. Criddle[b,g], Jesse D. Acosta[d], and Eric A. Appel[a,g,1]

[a]Department of Materials Science & Engineering, Stanford University, Stanford, CA 94305; [b]Department of Civil & Environmental Engineering, Stanford University, Stanford, CA 94305; [c]Department of Bioengineering, Stanford University, Stanford, CA 94305; [d]Department of Natural Resource Management & Environmental Sciences, California Polytechnic State University, San Luis Obispo, CA 93407; [e]Desert Research Institute, Reno, NV 89512; [f]Department of Chemistry, Stanford University, Stanford, CA 94305; and [g]Stanford Woods Institute for the Environment, Stanford University, Stanford, CA 94305

Edited by David A. Weitz, Harvard University, Cambridge, MA, and approved August 27, 2019 (received for review May 8, 2019)

Polyphosphate fire retardants are a critical tactical resource for fighting fires in the wildland and in the wildland–urban interface. Yet, application of these retardants is limited to emergency suppression strategies because current formulations cannot retain fire retardants on target vegetation for extended periods of time through environmental exposure and weathering. New retardant formulations with persistent retention to target vegetation throughout the peak fire season would enable methodical, prophylactic treatment strategies of landscapes at high risk of wildfires through prolonged prevention of ignition and continual impediment to active flaming fronts. Here we develop a sprayable, environmentally benign viscoelastic fluid comprising biopolymers and colloidal silica to enhance adherence and retention of polyphosphate retardants on common wildfire-prone vegetation. These viscoelastic fluids exhibit appropriate wetting and rheological responses to enable robust retardant adherence to vegetation following spray application. Further, laboratory and pilot-scale burn studies establish that these materials drastically reduce ignition probability before and after simulated weathering events. Overall, these studies demonstrate how these materials actualize opportunities to shift the approach of retardant-based wildfire management from reactive suppression to proactive prevention at the source of ignitions.

polymers | wildfire | viscoelastic | retardant | hydrogels

Every year in the United States, wildfires destroy millions of acres of forest, cost billions of dollars to suppress, and destroy the lives and livelihoods of thousands of people (1–4). While some wildfires are critical for healthy forest ecology, human activities cause 85% of fires in the United States, accounting for 44% of the total area burned, and have tripled the length of the fire season (2). Furthermore, numerous studies indicate that beyond incident casualties and infrastructure damage, wildfires lead to dangerous levels of airborne particulates that significantly increase risk of respiratory and cardiovascular diseases among human populations (5–10).

Yet, encouragingly, these wildfires predominantly initiate at select "high-risk" locations such as roadsides and utilities infrastructure, providing targets for prophylactic treatment efforts. California exhibits one of the most severe wildfires seasons worldwide and has the highest population living in the wildland–urban interface, where wildfires pose the greatest threat to human life (11). Approximately 84% of the 300,624 wildfires occurring in California over the past 10 years were initiated at these high-risk areas (Fig. 1 and *SI Appendix*, Table S1). Moreover, fires initiating at these high-risk areas are Tier 2 or Tier 3 threat regions (as designated by firefighting agencies) and are more severe and burn more acres per fire on average (Fig. 1*B*). These data suggest that treating these high-risk landscapes with retardant formulations that provide season-long protection against ignition could greatly reduce the incidence and severity of wildfires and, as a prophylactic strategy, allow for careful consideration of local factors before application.

Materials used for wildfire management are either categorized as fire suppressants or fire retardants, with many suppressants commonly used as short-term retardants. Fire suppressants are used for direct application onto an ongoing fire and include perfluorinated surfactant-based foams and "water-enhancing gels" based on superabsorbent polymers (12–20). Perfluorinated surfactant-based foams are highly effective at suppressing actively burning fires; however, they are classified as high-risk environmental contaminants because of their long-term environmental persistence, potential for bioaccumulation, and toxicity (21–23). Conversely, in addition to direct suppression of fires, water-enhancing gels have been used as short-term retardants on buildings in the path of encroaching fires (13–18). These gels are only effective when wet and do not stop fires once the water has evaporated, which often occurs in under an hour during normal wildland fire conditions (16, 24–26). As a result, these gels cannot be used for long-term preventative treatment of wildland fuels.

Significance

Despite strong fire prevention efforts, every year wildfires destroy millions of acres of forest. While fires are necessary for a healthy forest ecology, the vast majority are human-caused and occur in high-risk areas such as roadsides and utilities infrastructure. Yet, retardant-based treatments to prevent ignitions at the source are currently impossible with existing technologies, which are only suited for reactive fire prevention approaches. Here we develop a viscoelastic carrier fluid for existing fire retardants to enhance retention on common wildfire-prone vegetation through environmental exposure and weathering. These materials enable a prophylactic wildfire prevention strategy, where areas at high risk of wildfire can be treated and protected from ignitions throughout the peak fire season.

Author contributions: A.C.Y., H.L.H., A.H.K., L.M.S., C.S.C., J.D.A., and E.A.A. designed research; A.C.Y., H.L.H., A.H.K., L.M.S., R.J.B., E.T.M., C.P.B., D.C., J.D.A., and E.A.A. performed research; G.D.M. and A.J.W. contributed new reagents/analytic tools; A.C.Y., H.L.H., A.H.K., L.M.S., R.J.B., E.T.M., C.P.B., G.D.M., A.J.W., D.C., and E.A.A. analyzed data; and A.C.Y., H.L.H., and E.A.A. wrote the paper.

Conflict of interest statement: A.C.Y. and E.A.A. are listed as inventors on a patent describing the technology reported in this manuscript. On 25 October 2018, J.D.A. and E.A.A. founded a company called LaderaTECH, which has licensed the technology from Stanford University. All other authors declare no competing interests.

This article is a PNAS Direct Submission.

Data deposition: Data that support the results of this study are available within the paper and the Supporting Information. Additional relevant data are available upon request from the corresponding author.

[1]To whom correspondence may be addressed. Email: eappel@stanford.edu.

This article contains supporting information online at www.pnas.org/lookup/suppl/doi:10.1073/pnas.1907855116/-/DCSupplemental.

First published September 30, 2019.

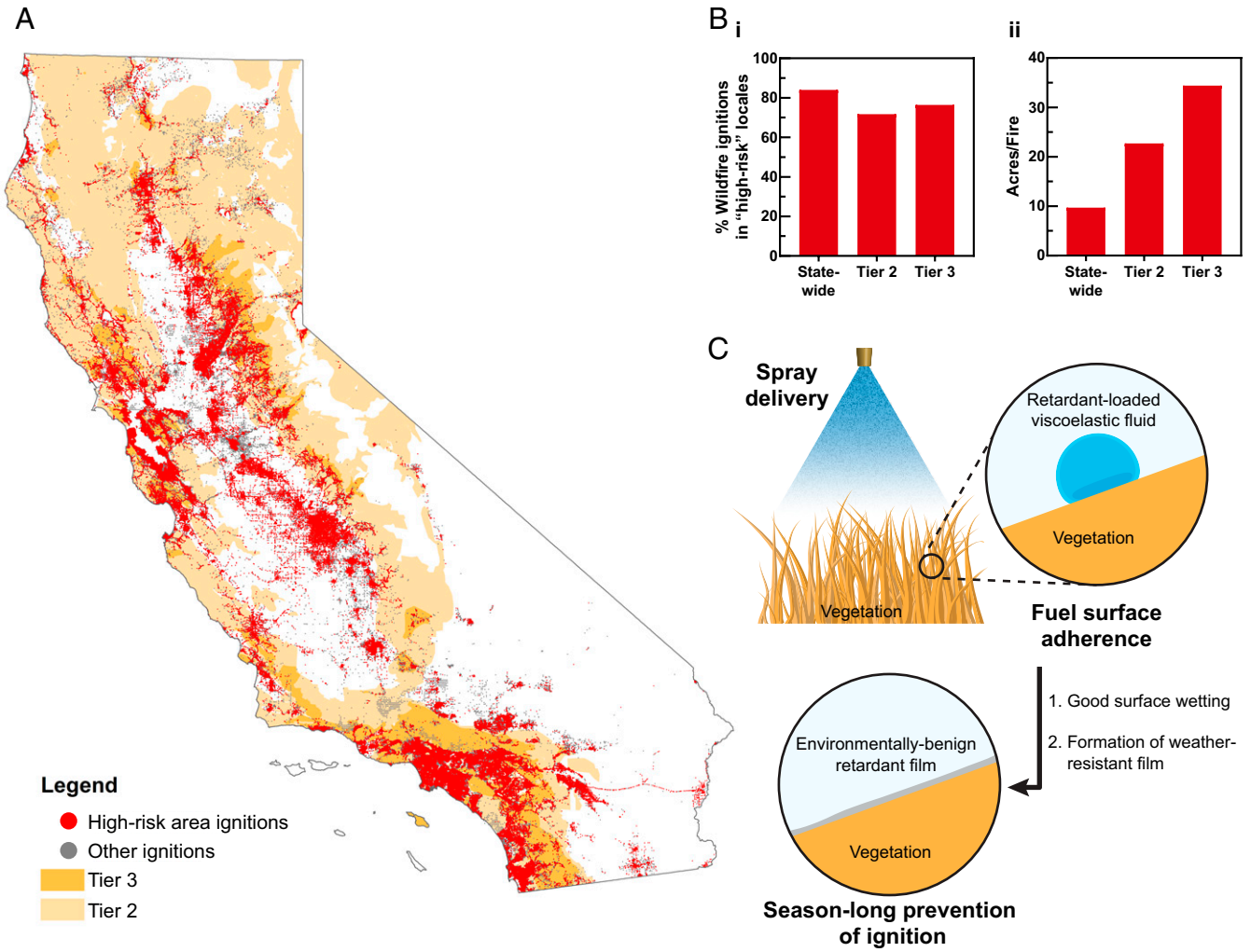

Fig. 1. Prophylactic treatment of landscapes at high risk of fire starts with environmentally benign polymer-particle retardant formulations. (*A*) Map of California displaying wildfires occurring between January 1, 2009 and December 31, 2018 with the fires initiating at high-risk locales (roadsides and utilities infrastructure) highlighted in red and fires initiating in all other locales shown in gray. Tier 2 and Tier 3 fire threat regions are highlighted in orange. (*B*) Bar plots exhibiting: 1) the percentage of ignitions occurring at high -risk locales throughout the entire state, and in Tier 2 and Tier 3 threat regions, and 2) the average number of acres burned per fire initiating in high-risk locales throughout the entire state, and in Tier 2 and Tier 3 threat regions. (*C*) Schematic of a prophylactic treatment strategy illustrating the spray delivery and adherence of a retardant-loaded viscoelastic fluid, followed by the formation of a weather-resistant, fire-retarding film.

On the other hand, fire retardants deemed "long-term retardants" use water primarily as a carrier medium for fire-retarding chemicals that maintain their efficacy even after drying (24–26). The "long-term" designation refers simply to the ability to maintain efficacy after drying and not the duration of their efficacy. The most widely deployed commercial wildland fire-retardant formulations use ammonium polyphosphate (APP) or ammonium phosphate as the active fire-retarding component mixed in aqueous formulations containing polymeric viscosity modifiers (i.e., guar gum and clay particles). In particular, Phos-Chek LC95A (PC) is the primary long-term retardant formulation used on natural wildland fuels (26, 27). Formulations such as PC are a primary tactical resource in fighting wildfires by reducing combustion efficiency and intumescing on the surface of vegetation to form a barrier against further fuel combustion (28, 29). More than 100 million gallons of these retardants are deployed annually to slow advancing flame fronts and to support crews in firebreak development (26, 27). Although the performance-enhancing additives in PC are useful for improving spread and reducing drift when dropped from aircraft during suppression efforts, they do not retain the retardants on target vegetation for extended periods of time, or through environmental exposure or weathering (e.g., rain or wind). As such, these materials cannot be used as preventative treatments to provide season-long protection against ignitions in natural wildland fuels.

Ultimately, existing fire retardants and suppressants are used only in emergency response efforts to mitigate the impact of ongoing wildfires and have failed to realistically provide a season-long preventative treatment due to unsuitable materials properties and/or environmental and health concerns (12–23).

Here, we report an environmentally benign cellulose-based viscoelastic fluid as a carrier for APP that improves adherence and retention on target vegetation and enables prolonged prevention of ignition in the wildland. These materials are formed through dynamic and multivalent polymer–particle (PP) interactions, whereby cellulose derivatives such as hydroxyethylcellulose (HEC) and methylcellulose (MC) adsorb onto colloidal silica particles (CSPs) in a multivalent, noncovalent manner (*SI Appendix*, Fig. S1) (30). Manufacturing of these materials is straightforward and inexpensive at large scales as they contain solely nontoxic starting materials widely used in food, drug, cosmetic, and agricultural formulations (30–33). Due to the noncovalent PP interactions, the viscoelastic fluids are shear-thinning and exhibit low thixotropy, allowing them

to be deployed with standard equipment for pumping or spraying used frequently in agricultural applications (Movie S1). We previously showed on the analytical scale that these materials can be used as carriers for APP fire retardants and may provide functional improvements over standard formulations (30). Here we demonstrate the prevention and suppression of wildfires on "light, flashy vegetation" and "1-h" vegetation at laboratory and pilot scale using PP materials loaded with APP. These PP materials do not have inherent fire-retarding effects and are solely used to enhance adherence and retention of APP (*SI Appendix*, Fig. S1). Wetting and rheological behavior are used to describe how PP materials enhance adherence of APP onto target vegetation during spray application and dry-film experiments demonstrate retention of APP through weathering. Lastly, we show that this combination of adherence and retention enables a preventative treatment strategy on landscapes at high risk for ignitions to reduce the incidence and severity of fire starts.

Results and Discussion

To successfully deploy, adhere, and retain fire retardant on vegetation, the PP material must exhibit properties that allow for spraying, uniform and stable wetting onto target vegetation, and film formation resistant to dissolution upon weathering (Fig. 1*C*). A series of different PP formulations (*SI Appendix*, Table S2) was prepared and their ability to meet these engineering criteria were determined through laboratory-scale spraying experiments, surface tension measurements, and rheometry.

From laboratory spray videos, it is immediately apparent that the commercial PC (LC95A) APP formulations partially wet and adhere poorly to target vegetation (grass) (Movie S2). In contrast, all PP formulations completely wet the vegetation upon spraying, resulting in a uniform film completely covering the target vegetation (Movies S3–S5). At equilibrium, the formation of small spherical islands (partial wetting) or a uniform film (wetting) is described by the spreading coefficient, $S = \gamma_{S0} - \gamma_{SL} - \gamma_{LV}$, where γ_{S0} is the surface tension of the dry substrate, γ_{SL} is the surface tension of solid–liquid interface, and γ_{LV} is the surface tension of the liquid–vapor interface (34, 35). When droplets are first in contact with the vegetation, if $S < 0$ the material will only partially wet the surface, limiting the surface coverage to islands of droplets as seen in the PC case. If $S \geq 0$, the droplets preferentially form stable films, which is ideal for uniformly coating vegetation with fire retardant, which is seen in all PP formulations. While γ_{SL} cannot be individually or directly measured for solid–liquid interfaces, γ_{LV} of each formulation was determined through stalagmometric methods (Fig. 2*A*). It is apparent that PC has a γ_{LV}~88 N/m, while all PP formulations exhibited lower values (55 to 80% of γ_{LV} determined for PC), suggesting the surface tension mediated increase in S may be responsible for the wetting differences. Furthermore, dynamic sessile drop measurements on grass also show evidence for the difference in wetting behavior for PC versus the PP formulations (*SI Appendix*, Fig. S3). While retraction of the PC droplet leads to a residual spherical cap with a stable contact angle indicative of a partially wetting state, formulations **1–5** all illustrate that retraction of the droplet leaves a flat film with a contact angle approaching zero, indicative of a wetting state.

Consistent with droplet-scale measurements, laboratory-scale spraying experiments on grass illustrated that all PP formulations exhibited enhanced adherence onto the vegetation over PC, whereby ~70% of the sprayed mass of formulations **1**, **3**, **4**, and **5** adhered on the vegetation (compare ~44% for PC; Fig. 2*B*). In the case of formulation **2**, only ~53% of the sprayed mass was retained on the vegetation, suggesting that surface tension is insufficient to fully explain the improved adherence. After the treated grass was oven-dried, weathering was simulated through spray application of water onto treated samples and the degree of fire-retardant (APP) retention on the vegetation was measured using inductively coupled plasma optical emission spectroscopy (ICP-OES) (Fig. 2*C*). While PC-treated samples lost ~33% of the adhered APP mass after only 0.25 inch (0.635 cm) of simulated weathering, **1**-treated samples completely retained the APP after simulated weathering with 0.5 inch (1.27 cm) of rainfall. These observations suggest dry film stability is critical for retention of APP on vegetation through weathering. This behavior was further qualitatively exemplified in water drop dissolution experiments on dried films of PC and **1**, and scanning electron microscopy (SEM; *SI Appendix*, Fig. S4). In water drop dissolution experiments, PC films eroded and/or delaminated after water dropping, while **1** completely maintained its film integrity under the same conditions (Fig. 2*D*). Furthermore, SEM images show that PC forms thinner films, with needle-like clumps that possibly contribute to easy delamination and flakiness (*SI Appendix*, Fig. S4*B*). On the other hand, SEM images of **1** treated grass exhibit thicker, more uniformly space-filling films (*SI Appendix*, Fig. S4*C*).

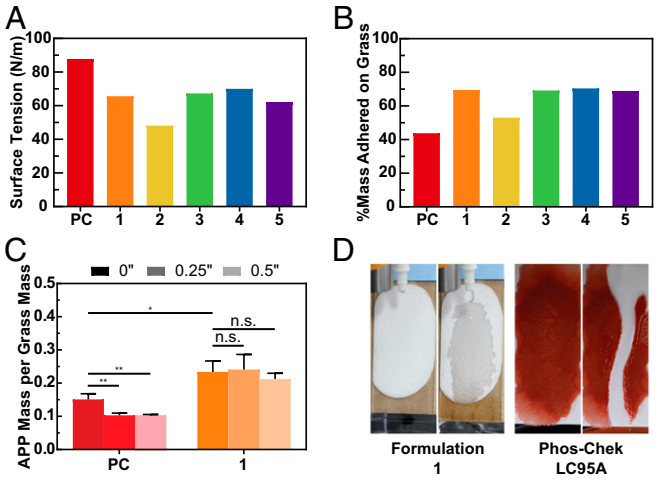

Fig. 2. Vegetation adherence and retention following spray application. (*A*) Surface tension values for each formulation. (*B*) Grass was treated by spray application of retardant formulations using a backpack sprayer and the mass adhered on the grass was measured. (*C*) The treated grass was blended and the phosphorus content was measured using ICP-OES. The mass of APP adhered per mass of grass before and following weathering with simulated rain events was calculated and plotted (mean ± SD; $n = 3$; 1-way analysis of variance within treatment groups $^{**}P < 0.01$, n.s. = not significant; unpaired t test for PC (0 inch) vs. **1** (0 inch) $^{*}P \leq 0.05$). (*D*) Stability of a dried film of **1** following simulated weathering by dropping water was visibly improved compared to a dried film of PC.

While the role of complex rheological properties on wetting, film formation, and adherence is an ongoing research topic (36–38), here we present the rheological behavior of each formulation and correlate it to coating efficiency and adherence onto vegetation. Rheological measurements of tan(δ) quantify the relative elasticity of each formulation, representing how liquid-like the material behaves at different timescales (Fig. 3*A* and *SI Appendix*, Fig. S2). Tan(δ) > 1 represents a more liquid-like response to stress (i.e., flows more easily for a given stress), while tan(δ) < 1 represents more solid-like behavior. PC and **2** display tan(δ) > 1 at lower angular frequencies, which represent longer timescales and thus relate to the materials' behavior after landing on the target vegetation. In contrast, all other PP formulations exhibit substantial solid-like properties at lower angular frequencies. Steady-shear measurements (Fig. 3*B*) show that every formulation is shear-thinning and, consistent with dynamic measurements, show that PC and formulation **2** require lower applied stresses for flow (Fig. 3*C*). The amount of stress required for formulations **1**, **3**, **4**, and **5** to flow at a given shear rate were all several-fold higher than required for flow of the more liquid-like PC and **2** to achieve the same shear rate. This comparison is also seen in dynamic yield stress values calculated

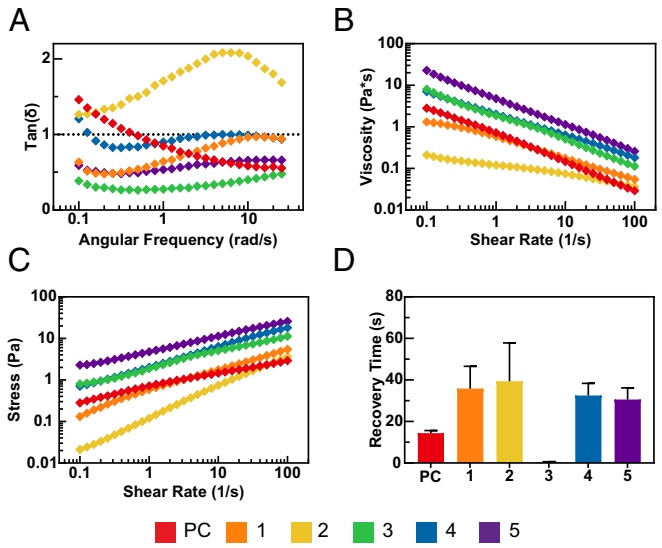

Fig. 3. Mechanical properties and interface properties. (*A*) Tan (δ) values obtained from oscillatory frequency sweeps characterizing the relative elasticity of each retardant formulation. (*B*) Steady-shear viscosity measurements of all retardant formulations. (*C*) Steady-shear viscosity measurements plotted as stress versus shear rate. (*D*) Structure recovery times determined from step-shear measurements (mean ± SD; $n = 3$).

from steady-shear experiments at low shear rates, where PC exhibits a dynamic yield stress of 0.005 Pa, which is 2 orders of magnitude smaller than any PP formulation (*SI Appendix*, Fig. S5). In agreement with the oscillatory rheometry, formulations **3**, **4**, and **5** have larger (~5- to 10-fold) dynamic yield stresses compared to **1** and **2** (*SI Appendix*, Fig. S5). Comparison of **1** and PC demonstrates that despite similar viscosities and shear-thinning profiles, the more solid-like (tan(δ) < 1) behavior of **1** at lower frequencies contributes, in addition to surface tension and dynamic yield stress, to the enhanced adherence to grass. These measurements suggest that viscosity alone does not contribute to enhance retention but that there may be a contribution from a solid-like response at lower frequencies to impede material flow following application.

The recovery rate of the solid-like network following shear was also investigated as it is important for the network to rapidly recover after spraying to maximize benefits of the formulations' viscosity and structure. Accordingly, it is advantageous that **1**, **3**, **4**, and **5** all shear-thin to allow for spraying, but also quickly recover their desired solid-like behavior due to their short network recovery times (Fig. 3*D* and *SI Appendix*, Fig. S6). Formulations **1**, **2**, **4**, and **5** exhibited similar, relatively longer recovery times, while **3** exhibited the shortest recovery time. In contrast, **2** exhibited the longest network recovery time of the PP formulations tested, likely exacerbating the poorer adherence observed previously. Interestingly, PC exhibited the fastest recovery time besides **3**, suggesting that despite the fast recovery time, the recovered structure is not optimal in relative elasticity, wetting, and yield stress for adherence as seen in the dynamic measurements.

As we propose to deploy these PP formulations in the wildland, it was critical to ensure they are environmentally benign, biodegrade at desired timescales, and are nontoxic. Formulation **1** prepared with cell media displayed no significant changes in apoptosis of adult human dermal fibroblast (HDFa) cells in culture when compared to an untreated control for the fully constituted formulation, as well as across all dilutions measured (Fig. 4*A*). To determine the aerobic and anaerobic biodegradability of these materials, we measured the biochemical oxygen demand (BOD) and the biochemical methane production (BMP), respectively, of the formulation with and without CSPs according to standard methods (39, 40). In BOD experiments, the PP mixtures did not exhibit any toxicity or inhibition of microbial activity as they reach the same dissolved oxygen concentration (~4 mg/L) as the blank after a 24-d period (Fig. 4*B*). Only the positive control consisting of glucose and glutamic acid showed significant oxygen depletion relative to the blank. Importantly, the absence of an additional oxygen demand for the PP formulations suggests that these materials would not contribute to organic pollution in the environment, which can place undue oxygen demand in surface waters within the watershed. In BMP experiments, both formulation groups produced modest amounts of methane [~14 L CH_4/kg chemical oxygen demand (COD)] at the end of the 30-d period, indicating that the materials do not inhibit methanogenic activity and are mildly resistant to biodegradation, and thus do not readily degrade when exposed to microbes (Fig. 4*C*). The slow rate of degradation can ensure local persistence on vegetation in the wildland over the timeframe of the high fire season, while the negligible aerobic degradation can prevent depletion of oxygen in the soil and watershed once the materials are washed away during season-ending weather events.

Laboratory-scale burn experiments were then used to assess the maintenance of fire-retardant function through weathering. Although burn experiments for consumer products (e.g., fabrics, plastics, etc.) are often performed in cone calorimeters, these methods are limited to small and typically flat samples and are unable to capture the dynamics of a spreading fire front typical of wildfires (41). Therefore, we established model burn chambers for each vegetation type of interest to more closely replicate at-scale burn dynamics and masses (*SI Appendix*, Fig. S7). Two vegetation types notorious for wildland fire starts were tested: 1) grass, which is a light, flashy vegetation and 2) chamise (greasewood) chipped to be a "1-h fuel" (41, 42). Treatments were performed according to standard retardant coverage levels (CLs) for each type of vegetation (i.e., CL1 ~0.41 L/m^2 for grass and CL2 ~0.82 L/m^2 for chamise) (43). Notably, these coverage levels would contribute insignificant amounts of soluble phosphorus to the environment upon application of these materials when compared to the 2- to 7-fold increase in watershed and soil phosphorus concentration due to dissolution of ash after a wildfire (44).

Grass burns were executed in burn chambers with a furnace ignitor at the base and a single chamber filled with treated grass, allowing for characterization of how well the treatments inhibit ignition and suppress spreading of fire (*SI Appendix*, Fig. S7*A*). The grass was burned after being treated with each formulation and weathered by simulating a rain event with 0, 0.25, or 0.5 inch (0, 0.64, or 1.27 cm) of water, reaching weathering in excess of what is typically experienced during a fire season. Integration of temperature–time curves for the burns represents the heat released (Fig. 5 *C*–*H*), illustrating that weathering dramatically reduced the retardant efficacy of PC, while negligibly affecting the efficacy of **1** (Fig. 5 *A*–*H* and *SI Appendix*, Fig. S8 *A*–*C*). These data are in agreement with laboratory-scale mass adherence and retention experiments described above (Fig. 2 *B* and *C*). In these experiments, 100% performance was defined as the behavior of the PC-treated grass without weathering. The performance of PC-treated grass drops to ~60% after 0.25 inch of rain and becomes similar to untreated grass after 0.5 inch of rain (Fig. 5*A*). Notably, **1**-treated grass without weathering exhibited essentially no ignition among the samples tested, resulting in no appreciable heat released or mass consumed and a burn performance of ~130% (Fig. 5*A*). From the materials characterization of PC and **1**, we hypothesize that the enhanced wetting, recovery time, and solid-like behavior of **1** maximize adherence of the formulations on the grass, while the film-phase stability of **1** enhances retention on the grass through weathering. All other PP formulations exhibited enhanced weather resistance over PC but did not perform as well as **1**. Consequently, **1** was chosen for all subsequent pilot-scale burn experiments due to its unique combination

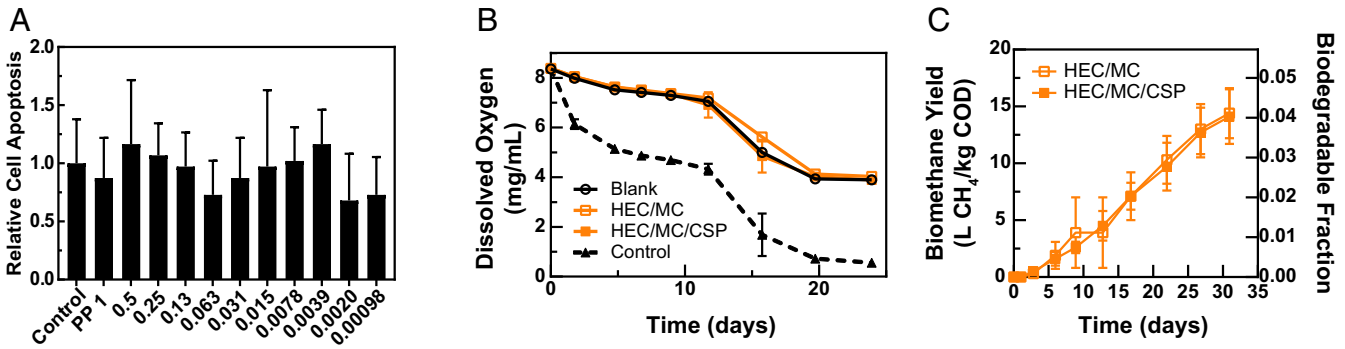

Fig. 4. Cytotoxicity, biocompatibility, and biodegradability. (*A*) Cytotoxicity experiments of PP formulation 1 at different dilutions exhibiting the relative cell apoptosis compared with an untreated control using HDFa cells (mean ± SD; $n = 8$). (*B*) BOD measurements (mean ± SD; $n = 3$) illustrating the materials to be environmentally benign as these materials do not aerobically degrade and do not inhibit aerobic degradation processes. The abrupt decrease in dissolved oxygen observed for all samples at day 12 is due to ammonium oxidation. (*C*) BMP experiments (mean ± SD; $n = 3$), plotted as liters of methane per kilogram of COD, illustrating slow anaerobic degradation of the PP formulation, enabling persistence in the wildland over the timeframe of the peak fire season.

of favorable spray characteristics, rheological properties, wetting and adherence capability, and resistance to weathering.

Chamise (greasewood) burns were executed in burn chambers split into a bottom chamber filled with untreated chips and a top chamber filled with treated chips to characterize how well fire carries into the treated fuel (*SI Appendix*, Fig. S7*B*). Notably, chamise is known to have higher effective heats of combustion and peak heat release rates when compared to other types of vegetation in California (41). Based on our previous experiments in grass, we assessed the performance of PP formulations **1** and **5** in comparison to PC. Formulation **5** was chosen as a counterpoint to **1** because **5** represents the highest concentration PP formulation. Similar to our previous experiments, we found that weathering significantly reduced the ability for PC to suppress the spread of fire, resulting in a faster burn rate, while the performance of both **1** and **5** was maintained through weathering (Figs. 2*B* and

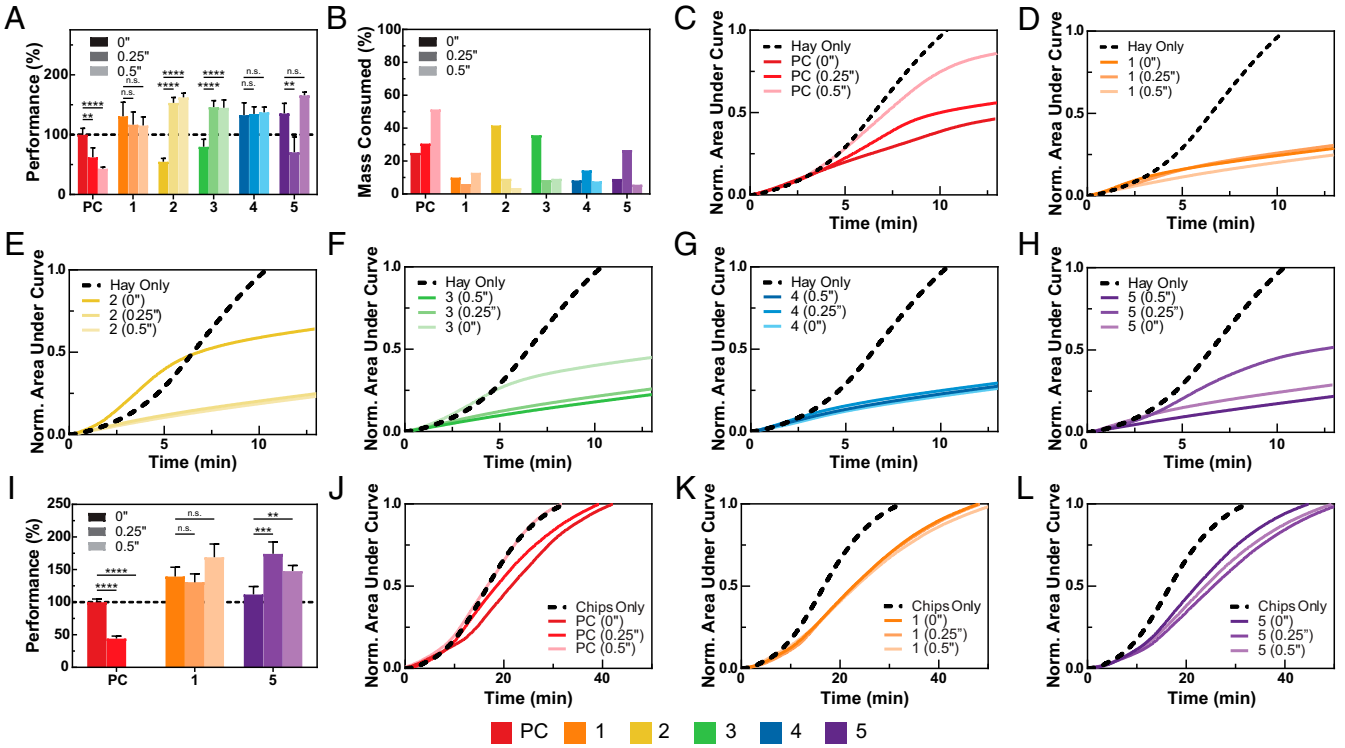

Fig. 5. Laboratory-scale grass burn experiments. (*A*) Normalized performance of each treatment (mean ± SD; $n = 4$; 1-way analysis of variance $^{**}P < 0.01$, $^{***}P < 0.001$, $^{****}P < 0.0001$). In these experiments, 100% performance was defined as the total area under the temperature–time curve of PC-treated grass without weathering. Performance for each formulation is calculated as $\frac{\text{Area under the curve of test formulation}}{\text{Area under the curve of PC without weathering}}$. (*B*) The mass after each burn demonstrates a significant decrease in the total mass burned for each PP treatment. Markedly, formulations 2 and 3 exhibited a decrease in mass consumed after being rained on, possibly due to spreading of the formulation due to rain. (*C–H*) Plots of normalized area under the temperature vs. time curves for each formulation compared to the untreated grass (data shown are the mean of $n = 4$). (*I*) Normalized performance of each treatment (mean ± SD; $n = 4$; 1-way analysis of variance $^{**}P < 0.01$, $^{***}P < 0.001$, $^{****}P < 0.0001$), where 100% performance was defined as the total area under the temperature–time curve of PC-treated chamise chips without weathering. Performance for each formulation is calculated as $\frac{\text{Area under the curve of test formulation}}{\text{Area under the curve of PC without weathering}}$. (*J–L*) Plots of normalized area under the temperature vs. time curves for each formulation compared to the untreated chamise chips (data shown is the mean of $n = 4$).

5 *I–L*, and *SI Appendix*, Fig. S8 *D–F*). Again, we defined 100% performance as the behavior of the PC-treated chips without weathering. Weathering of PC-treated chamise chips resulted in a performance drop to <50% after 0.25 inch of simulated rain, while PC treatment performed no better than untreated chamise chips after 0.5 inch of simulated rain. Yet, for fuel treated with **1** and **5**, the efficacy remained consistent even after 0.5 inch of rain (Fig. 5 *K* and *L*). Similar to grass, chamise chips treated with PP formulations exhibited superior performance to PC (~140%) on account of enhanced retardant adherence and retention following application (Fig. 5 *I*, *K*, and *L*).

With a clear improvement of **1** over PC, we tested the coverage level of **1** needed to minimize burning in pilot-scale plots (3 m × 3 m) of mowed and unmowed (standing) dry grass (both are characteristic of high-risk landscapes in many locations within the high fire-threat regions described above; *SI Appendix*, Fig. S9) and chamise piles (~100 kg of material) alongside firefighters from Cal Fire San Luis Obispo. Following spray application of **1** on mowed grass without weathering, we observed that flame is stopped immediately after ignition in plots treated at only CL1, while >90% of the area in untreated control plots burned within 60 s (*SI Appendix*, Fig. S10 and Movie S9). After weathering with 0.5 inch of rain on each coverage level, results indicate that while CL2 dramatically reduced the rate of spread of the flaming front, CL3 or higher is necessary to completely prevent the spread of the flame (Fig. 6*A*, *SI Appendix*, Fig. S11, and Movies S10 and S11). These results indicate that CL1 is sufficient to completely stop the spread of fire on mowed grass when directly applied, while CL3 is sufficient for complete protection through weathering. Analogously, standing grass burns illustrated that >90% of the area of untreated control plots burned within 60 s, while treatment at CL2 was sufficient to completely stop the active flaming front after weathering (Fig. 6*B* and Movies S12 and S13).

In addition to pilot-scale burns with grass, we conducted burns with chamise piles (100 kg of material; Fig. 6*C* and *SI Appendix*, Fig. S12). The piles were treated with CL3 of formulation **1**, weathered (0.5 inch of simulated rain), and thoroughly dried through environmental exposure prior to burning. All burns were started by ignition of an untreated starter bundle of chamise (1 kg; *SI Appendix*, Fig. S12*A*). Untreated control piles rapidly ignited and grew to a steady-state burn temperature after ~110 s, while **1**-treated piles exhibited delayed ignition and slower flame growth until ~400 s, corresponding to an ~4× decrease in the rate of spread (as indicated by the slope of the burn profiles) compared with the control group (Fig. 6*C* and *SI Appendix*, Fig. S12*C*). The slower rate of ignition and transition of the flame from the untreated starter bundle to the treated pile is due to the intumescent effects of the ammonium polyphosphate in **1**. Nonetheless, for these pilot-scale burns, the impact of the fire retardants was largely observed during the early phase of the burns. Once the fires mature (>420 s), the heat release overcomes the intumescent effects of the applied retardants and the piles proceed to burn normally, resulting in similar flame sizes and average temperatures across all treatments.

Conclusion

Overall, we have demonstrated that HEC/MC/CSP viscoelastic fluids can be engineered to exhibit viscoelastic fluid-phase and film-phase materials properties that support uniform application, adherence, and retention of polyphosphate fire retardants onto target wildland vegetation. Crucially, these materials are created from biodegradable and nontoxic starting materials through a facile and scalable manufacturing process (*SI Appendix*, Fig. S13). This combination of material properties allows for prevention of seasonal attrition of fire-retardant coverage induced by weathering or premature microbial degradation and enable a prophylactic treatment strategy to prevent wildfires on landscapes at high risk for fire starts. We propose that the utilization of such a strategy will reduce the incidence and severity of wildfire to protect critical infrastructure and the lives and livelihoods of people in wildfire-prone regions.

Methods

Materials. HEC (molecular weight ~ 1,300 kDa) and MC (molecular weight ~ 90 kDa) were obtained from Sigma-Aldrich. CSPs (Ludox TM-50; diameter ~ 15 nm) were obtained from Sigma-Aldrich. APP was obtained from Sigma-Aldrich or from Parchem. PC was provided by Phos-Chek.

California Wildfire Map. Map and associated fire ignition data were gathered from California ignition data from January 1, 2009 through December 31, 2018 available through the Fire and Resource Assessment Program (FRAP) database. The number of total wildfires excludes structure fires. Tier 2 threat regions represent areas with elevated risk of impact on people and property from a wildfire and total 37,023,418 acres in the state of California. Tier 3 threat regions represent areas with extreme risk of impact on people and property from a wildfire and total 7,988,148 acres in the state of California. Complete data are presented in *SI Appendix*, Table S1.

Polymer-Particle Viscoelastic Fluid Formation. Polymer-particle formulations were prepared according to previously described methods (30). The concentrations used were 0.1 or 0.2 wt % HEC/MC (0.85/0.15) with 0.5, 1, or 2 wt % CSP, and 13.5 wt % APP.

Dynamic and Flow Rheometry. All rheometry experiments were performed on a torque-controlled Discover HR2 Rheometer (TA Instruments) using a 60-mm cone plate (2.007°) geometry. Frequency sweeps were conducted in the linear viscoelastic regime from 0.1 to 100 rad/s. Steady-shear experiments were performed from 0.1 to 100 s^{-1}. Step-shear experiments were performed alternating between 100 and 0.2 s^{-1}. Low shear-rate steady-shear experiments were performed from 1 to 10^{-5} s^{-1} and dynamic yield stresses were calculated using the Herschel–Bulkley equation for points up to 10^{-2}·s^{-1}.

Biodegradability Studies. The COD and BOD of the HEC/MC and HEC/MC/CSP mixtures were determined according to standard methods (39).

Laboratory Water Drop Test. One mL of PC or of each PP material formulated with ammonium polyphosphate was pipetted onto a glass slide and allowed to dry overnight. These glass slides were then placed at an ~50° incline and water was dripped onto the dried sample from a nozzle ~1.3 cm above the slide in a controlled manner using a syringe pump. The syringe pump was set at a flow rate of 5 mL/min and a total of 20 mL of water was applied. A Canon EOS REBEL T5i/EOS 700D DSLR camera was used to take videos and images.

Laboratory Spray Experiments. Each formulation (100 mL) was loaded into a backpack sprayer (Field King) and sprayed onto a layer of grass taped to a wood slab. The nozzle was placed ~30 cm away from the grass and sprayed in bursts. The videos were captured using a Canon EOS REBEL T5i/EOS 700D DSLR camera.

Laboratory Treatment Retention Experiments. Grass (150 g) was spread out and spray-treated with **1** or PC (200 g). The mass of the runoff was measured. The treated grass was then dried to a consistent weight. The final weight of the grass was measured and compared to the untreated control to quantify the amount of treatment adhered on the vegetation. Treated vegetation (20 g) was then weathered with either 0, 0.25, or 0.5 inch (0, 445, or 889 mL) of simulated rainfall and then dried. The grass samples were then homogenized by grinding, dissolved in piranha solution (3:1 sulfuric acid: hydrogen peroxide), and the phosphorus content was determined using ICP-OES.

Laboratory-Scale Grass Burn Experiments. Grass burn chambers (*SI Appendix*, Fig. S7*A*; $n = 4$) were loaded with treated, weathered, and dried grass (30 g). The chamber ignitor was heated to 250 °C and the thermocouple temperatures were monitored over time. At the end of the burn, samples were allowed to cool to ambient temperature and the total mass of remaining sample was recorded.

Laboratory-Scale Chamise Chip Burn Experiments. Chamise chip burn chambers (*SI Appendix*, Fig. S7*B*; $n = 4$) were loaded with treated, weathered, and

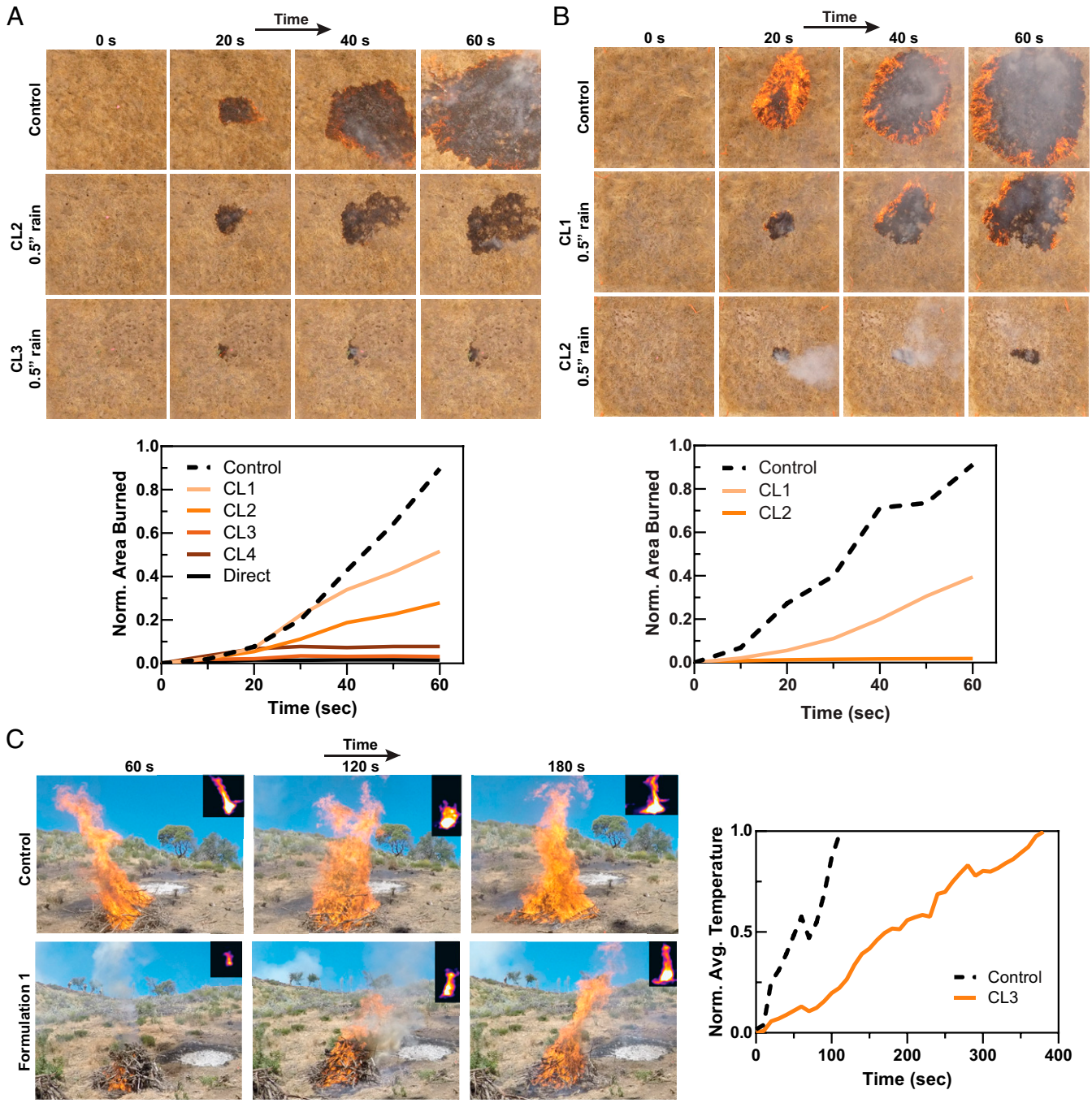

Fig. 6. Pilot-scale burn studies in treated and weathered grass and chamise. (*A*) Overhead time-course images of mowed grass plots untreated or treated with different coverage levels of **1**. Treated plots were allowed to dry completely over the course of ∼2 wk (exposing the sites to the environment as they dry) prior to weathering (0.5 inch of simulated rainfall), then allowed to dry completely over the course of ∼2 wk prior to burning. The normalized area burned demonstrates that coverage level 3 is sufficient to preclude spreading of the fire. (*B*) Overhead time-course images of 3 m × 3 m unmowed (standing) grass plots that were untreated or treated with different coverage levels of **1**, dried, weathered, and allowed to dry again over time in the environment prior to burning. The normalized area burned over time demonstrates that coverage level 2 is sufficient to preclude spreading of the fire. (*C*) Images of pilot-scale burns of chamise piles with infrared (IR) image overlays. Chamise was treated at CL3, dried completely through environmental exposure, weathered (0.5 inch of simulated rainfall), dried through environmental exposure again, and then burned. The temperature–time curves extracted from IR images taken over time were integrated and normalized to the plateau burn temperature of the untreated control pile, indicating that weathered treated chamise exhibited an ∼4× decrease in burn rate compared to controls.

dried chips (1 kg) placed into the top section of each burn chamber, with untreated chips (500 g) placed in the bottom. The untreated vegetation was ignited and the thermocouple temperatures were monitored over time.

Pilot-Scale Grass Burn Experiments. Grass plots (3 m × 3 m) that were either mowed or unmowed to simulate roadside conditions were treated (leaving a center circle untreated), allowed to dry, weathered, and dried again. The center of each plot was ignited with a hand torch and the burn area was monitored with a drone (DJI; Phantom 3 Professional).

Pilot-Scale Chamise Burn Experiments. Chamise was treated, allowed to dry, weathered, and dried again. Chamise piles (1 m × 1 m) were ignited from a

starter bundle and the burn was monitored using both a normal camera and an infrared camera (FLIR; Vue Pro-336).

ACKNOWLEDGMENTS. We thank Alan Peters (Division Chief) and David Fowler (Fire Captain, prefire engineering) from Cal Fire San Luis Obispo, and Daniel Turner from the San Luis Obispo County Fire Safe Council for helpful discussions and providing safety support during large-scale burns. We thank Ashley Fisher, Hannah K. Panno, and David Fowler from Cal Fire San Luis Obispo for help gathering and analyzing fire ignition data for the state of California from the FRAP. We thank David Kempken (Support Shop Manager) for technical support in burn chamber development. We would also like to thank FLIR for providing access to the Vue Pro 336 infrared camera. Part of this work was performed at the Stanford Nano Shared Facilities, supported by the National Science Foundation (NSF) under Award ECCS-1542152. This work was supported by a Kodak Fellowship (A.C.Y.), NSF Alliances for Graduate Education and the Professoriate (AGEP) Fellowship (H.L.H.), and a Realizing Environmental Innovation Program Grant from the Stanford Woods Institute for the Environment.

1. United States National Interagency Fire Center, Historical wildland fire information. https://www.nifc.gov/fireInfo/fireInfo_statistics.html. Accessed 1 August 2018.
2. J. K. Balch *et al*., Human-started wildfires expand the fire niche across the United States. *Proc. Natl. Acad. Sci. U.S.A.* **114**, 2946–2951 (2017).
3. V. C. Radeloff *et al*., Rapid growth of the US wildland-urban interface raises wildfire risk. *Proc. Natl. Acad. Sci. U.S.A.* **115**, 3314–3319 (2018).
4. C. I. Millar, N. L. Stephenson, S. L. Stephens, Climate change and forests of the future: Managing in the face of uncertainty. *Ecol. Appl.* **17**, 2145–2151 (2007).
5. C. E. Reid *et al*., Critical review of health impacts of wildfire smoke exposure. *Environ. Health Perspect.* **124**, 1334–1343 (2016).
6. J. C. Liu, G. Pereira, S. A. Uhl, M. A. Bravo, M. L. Bell, A systematic review of the physical health impacts from non-occupational exposure to wildfire smoke. *Environ. Res.* **136**, 120–132 (2015).
7. T. C. Wegesser, K. E. Pinkerton, J. A. Last, California wildfires of 2008: Coarse and fine particulate matter toxicity. *Environ. Health Perspect.* **117**, 893–897 (2009).
8. A. Haikerwal *et al*., Impact of fine particulate matter ($PM_{2.5}$) exposure during wildfires on cardiovascular health outcomes. *J. Am. Heart Assoc.* **4**, e001653 (2015).
9. J. C. Liu *et al*., Wildfire-specific fine particulate matter and risk of hospital admissions in urban and rural counties. *Epidemiology* **28**, 77–85 (2017).
10. C. D. McClure, D. A. Jaffe, US particulate matter air quality improves except in wildfire-prone areas. *Proc. Natl. Acad. Sci. U.S.A.* **115**, 7901–7906 (2018).
11. S. Martinuzzi *et al*., *The 2010 Wildland-Urban Interface of the Conterminous United States* (U.S. Department of Agriculture, Forest Service, Northern Research Station, Newton Square, PA, 2015).
12. E. Kissa, *Fluorinated Surfactants: Synthesis, Properties, Applications* (Dekker, New York, 1994).
13. D. Schoeder, *Can Fire Suppressant Gels Protect Log Decks? A Case Study to Test the Concept* (Forest Engineering Research Institute of Canada, Vancouver, 2006).
14. D. Schoeder, *Can Fire Suppressant Gels Protect Log Decks? Part III - Two Case Studies to Test Gel Effectiveness Against Radiant and Convective Heat Transfer* (Forest Engineering Research Institute of Canada, Vancouver, 2006).
15. D. Schoeder, *Effectiveness of Forest Fuel Management: A Crown Fire Case Study in the Northwest Territories, Canada* (Forest Engineering Research Institute of Canada, Vancouver, 2006).
16. United States Forest Service, Water enhancers for wildland fire management. https://www.fs.fed.us/rm/fire/documents/2019%20qpl_we_2019-May.pdf. Accessed 1 June 2019.
17. C. M. Bordado, F. P. Gomes, New technologies for effective forest fire fighting. *Int. J. Environ. Stud.* **64**, 243–251 (2007).
18. R. N. Bashaw, B. G. Harper, "Method for controlling the spread of fire." US Patent 3229769A (1963).
19. J. E. Pascente, T. J. Pascente, "Method of preventing combustion by applying an aqueous superabsorbent polymer composition." US Patent 5849210A (1995).
20. N. Seetapan, N. Limparyoon, S. Kiatkamjornwong, Effect of fire retardant on flammability of acrylamide and 2-acrylamido-2-methylpropane sodium sulfonate copolymer composites. *Polym. Degrad. Stabil.* **96**, 1927–1933 (2011).
21. C. A. Moody, G. N. Hebert, S. H. Strauss, J. A. Field, Occurrence and persistence of perfluorooctanesulfonate and other perfluorinated surfactants in groundwater at a fire-training area at Wurtsmith Air Force Base, Michigan, USA. *J. Environ. Monit.* **5**, 341–345 (2003).
22. C. A. Moody, J. A. Field, Perfluorinated surfactants and the environmental implications of their use in fire-fighting foams. *Environ. Sci. Technol.* **34**, 3864–3870 (2000).
23. X. C. Hu *et al*., Detection of poly- and perfluoroalkyl substances (PFASs) in U.S. drinking water linked to industrial sites, military fire training areas, and wastewater treatment plants. *Environ. Sci. Technol. Lett.* **3**, 344–350 (2016).
24. A. Agueda, E. Pastor, E. Planas, Different scales for studying the effectiveness of long-term forest fire retardants. *Pror. Energy Combust. Sci.* **34**, 782–796 (2008).
25. Phos-Chek, Phos-chek INSUL-8 water enhancing gel. https://phoschek.com/product/phos-chek-insul-8-wildland/. Accessed 1 June 2019.
26. A. Gimenez, E. Pastor, L. Zárate, E. Planas, J. Arnaldos, Long-term forest fire retardants: A review of quality, effectiveness, application and environmental considerations. *Int. J. Wildland Fire* **13**, 1–15 (2004).
27. United States Forest Service, Nationwide aerial application of fire retardant on national forest system land. https://www.fs.fed.us/sites/default/files/media_wysiwyg/wfcs_final_feis_0.pdf. Accessed 1 June 2019.
28. J. Green, A review of phosphorus-containing flame retardants. *J. Fire Sci.* **10**, 470–487 (1992).
29. G. Camino, L. Costa, L. Trossarelli, Study of the mechanism of intumescence in fire retardant polymers: Part V—Mechanism of formation of gaseous products in the thermal degradation of ammonium polyphosphate. *Polym. Degrad. Stabil.* **12**, 203–211 (1985).
30. A. C. Yu *et al*., Scalable manufacturing of biomimetic moldable hydrogels for industrial applications. *Proc. Natl. Acad. Sci. U.S.A.* **113**, 14255–14260 (2016).
31. D. G. Coffey, D. A. Bell, A. Henderson, "Cellulose and cellulose derivatives" in *Food Polysaccharides and Their Applications*, A. M. Stephen, Ed. (Marcel Dekker Inc., New York, 1995), pp. 123–154.
32. T. K. Barik, B. Sahu, V. Swain, Nanosilica-from medicine to pest control. *Parasitol. Res.* **103**, 253–258 (2008).
33. E. Dickinson, Food emulsions and foams: Stabilization by particles. *Curr. Opin. Colloid Interface Sci.* **15**, 40–49 (2010).
34. P. G. De Gennes, Wetting: Statics and dynamics. *Rev. Mod. Phys.* **57**, 827–863 (1985).
35. D. Bonn, J. Eggers, J. Indekeu, J. Meunier, E. Rolley, Wetting and spreading. *Rev. Mod. Phys.* **81**, 739–805 (2009).
36. J. H. Snoeijer, B. Andreotti, Moving contact lines: Scales, regimes, and dynamical transitions. *Annu. Rev. Fluid Mech.* **45**, 269–292 (2013).
37. D. Izbassarov, M. Muradoglu, Effects of viscoelasticity on drop impact and spreading on a solid surface. *Phys. Rev. Fluids* **1**, 023302 (2016).
38. R. Lhermerout, H. Perrin, E. Rolley, B. Andreotti, K. Davitt, A moving contact line as a rheometer for nanometric interfacial layers. *Nat. Commun.* **7**, 12545 (2016).
39. E. W. Rice, R. B. Baird, A. D. Eaton, *Standard Methods for the Examination of Water and Wastewater* (American Public Health Association, American Water Works Association, and Water Environmental Federation, Washington, DC, 2017).
40. R. A. Labatut, L. T. Angenent, N. R. Scott, Biochemical methane potential and biodegradability of complex organic substrates. *Bioresour. Technol.* **102**, 2255–2264 (2011).
41. M. A. Finney *et al*., Role of buoyant flame dynamics in wildfire spread. *Proc. Natl. Acad. Sci. U.S.A.* **112**, 9833–9838 (2015).
42. R. H. White, D. R. Weise, K. Mackes, A. C. Dibble, "Cone calorimeter testing of vegetation: An update" in *Proceedings of the International Conference on Fire Safety* (US Forest Service, 2002), vol. 35.
43. United States Forest Service, Coverage levels. https://www.fs.fed.us/rm/fire/pubs/pdfpubs/user_gd/ug-06.pdf. Accessed 1 August 2018.
44. A. J. Ranalli, "A summary of the scientific literature on the effects of fire on the concentration of nutrients in surface waters" (US Geological Survey Open-File Report 2004-1296, 2004).